PCCP

Accepted Manuscript

This is an *Accepted Manuscript*, which has been through the Royal Society of Chemistry peer review process and has been accepted for publication.

Accepted Manuscripts are published online shortly after acceptance, before technical editing, formatting and proof reading. Using this free service, authors can make their results available to the community, in citable form, before we publish the edited article. We will replace this *Accepted Manuscript* with the edited and formatted *Advance Article* as soon as it is available.

You can find more information about *Accepted Manuscripts* in the **Information for Authors**.

Please note that technical editing may introduce minor changes to the text and/or graphics, which may alter content. The journal's standard **Terms & Conditions** and the **Ethical guidelines** still apply. In no event shall the Royal Society of Chemistry be held responsible for any errors or omissions in this *Accepted Manuscript* or any consequences arising from the use of any information it contains.

ARTICLE TYPE

Gluing together metallic and covalent layers to form Ru$_2$C at ambient conditions

Weiwei Sun[*a,b], **Yunguo Li**[†a], **Zhu Li**[c], **Yanming Ma**[c], **Igor Di Marco**[b], **Börje Johansson**[a,b] and **Pavel Korzhavyi**[a]

DOI: 10.1039/b000000x

Ru$_2$C has recently been synthesised under high pressure and high temperature, and was assumed to have a structure with space group $P\bar{3}m1$. However, subsequent theoretical work has revealed that this structure is unstable at ambient conditions, which motivates us to look for the stable structure. In this work, we explore the structures of Ru$_2$C by using an unbiased swarm structure searching algorithm. The structures with $R3m$ and $R\bar{3}m$ symmetry have been found to be lower in energy than the $P\bar{3}m1$ structure, being at the same time dynamically stable at ambient conditions. These layered structures are with alternating Ru bilayers and C monolayers for the $R3m$ structure, and alternating Ru tetra-layers and C bilayers for the $R\bar{3}m$ structure. The C layers are more evenly distributed and more covalently bound to the Ru layers in the $R3m$ structure than in the $R\bar{3}m$ structure. Instead, in the $R\bar{3}m$ structure there exists more Ru-Ru metallic bonding, which has a crucial role in diminishing the hardness of this material. Our findings should stimulate further explorations of the structures and properties of the heavy transition metal carbides and nitrides, potentially leading to industrial applications.

1 Introduction

Searching for materials with exotic hardness has been one of the long-standing activities in materials science. Superhard materials are usually composed of covalent light elements and synthesized under high-pressure conditions, and a well-known example is the cubic boron nitride (c-BN)[1,2]. The combination of light elements (like B, C, N or O) with valence electron-rich transition metals (like Ta, W, Re, Os or Ru) offers an alternative route to synthesize superhard materials.[3–5] In fact, some transition metal carbides (TMCs) and nitrides (TMNs) are already used for industrial applications, owing to their outstanding hardness, high melting point and corrosion resistance[6]. This type of synthesis essentially depends on the formation of p-d hybridised covalent bonds between the light elements and transition metals (TMs). The basic principle is that TMs contribute to the high hardness by providing a large number of valence electrons to the compounds. However, it is observed that the formation of late TMCs/TMNs is not so favourable due to the higher formation energies of the heavier TMs in comparison with lighter TMs[7,8]. To overcome this problem, one can apply an external pressure in the process of the synthesis, in order to enhance their chemical activities. The successful high-pressure synthesis of Re$_2$C[9], OsN$_2$[10] and Re$_2$N[11] is the highlight of this approach, illustrating that the applied pressure can overcome high formation energy barriers. More recently, Ru$_2$C has been synthesised successfully at high pressure and high temperature[12], and then it was brought back to ambient conditions. However, the X-ray diffraction (XRD) peaks between 18° and 22° experience a sudden change between 2.4 GPa and 0 GPa. Hence, a phase transition in the experiment is likely to occur during the quenching from extreme conditions to ambient conditions. The subsequent theoretical study[13] shows that the proposed structure with $P\bar{3}m1$ symmetry is unstable at ambient conditions but can be stabilised above 30 GPa through a Lifshitz transition. It is noticed that the experimental structure was obtained by fitting the simulated XRD patterns of some known $3d$ TMCs/TMNs to the measured XRD patterns. In fact, the structures of light TMCs/TMNs are supposed to differ from the heavy $4d$ counterparts because the $4d$ bands are significantly broader than the $3d$ bands. Therefore, more studies of the late TMCs/TMNs are necessary to firmly establish their structures and properties, which will set up a scientific basis for the development of this new family of hard materials.

There is no doubt that determining the crystal structure of a crystalline solid is an essential prerequisite for understanding and possibly exploiting its physical properties. The thermodynamic ground state of a material usually corresponds to the global minimum of the free energy surface. It is truly a minimisation problem, and can be solved by searching among all structures for the one with the lowest energy. However, a direct comparison is often too cubersome to be feasible, even for a system containing only one or two atoms per unit cell.

[a]*Department of Material Science and Engineering, KTH - Royal Institute of Technology, Stockholm SE - 10044, Sweden; E-mails: *provels8467@gmail.com, †yunguo@kth.se*

[b]*Department of Physics and Astronomy, Material theory, Uppsala University, Box 516, SE - 75120 Uppsala, Sweden; E-mail: *provels8467@gmail.com*

[c]*State Key Laboratory of Superhard Materials, Jilin University, Changchun 130012, People's Republic of China*

Therefore this task has been addressed using heuristic optimisations. Up to now, evolutionary algorithms and particle swarm optimisations are among the most used heuristic algorithms and have been recently established as reliable methods for crystal structure predictions [14–18].

The search for low-energy crystalline structures of Ru_2C was performed through the CALYPSO code [17,18] based on the particle swarm optimisation (PSO) algorithm. The whole procedure is unbiased by any prior information on the known structures. Recent successful applications of this method include various crystalline systems, ranging from elemental solids to binary and ternary compounds [19,20], and TMCs/TMNs [21,22]. As far as we know, the stable TMCs/TMNs and the high pressure stable phase ($P\bar{3}m1$) mostly crystallise in a primitive cell containing one or two formula units (f.u.). Therefore, the cutoff of the number of f.u. per primitive cell goes up to two in this study. Regarding the structures, CALYPSO found two trigonal crystalline structures, with space group $R3m$ (1 f.u.) and $R\bar{3}m$ (2 f.u.), respectively. By also considering the previously proposed structure ($P\bar{3}m1$ symmetry), the $R\bar{3}m$ structure has been identified as the most energetically favoured structure at zero pressure. Moreover, both these predicted structures are dynamically stable at ambient conditions. Thus we identify two metastable phases in the Ru-C binary system that may be prototype structures for other later TMCs/TMNs. Our main finding is that Ru_2C is constructed by bilayers of Ru and monolayers of C for the $R3m$ phase and tetra-layers of Ru and bilayers of C for the $R\bar{3}m$ phase. The XRD patterns of the predicted structures are simulated and compared with the experimental data. The electronic structure and the nature of the chemical bonding are also analysed here. Unlike the common TMCs, metallic bonds in the $R\bar{3}m$ phase are observed, which supplies a new mechanism to form heavy TMCs/TMNs. However, these bonds lead also to a strong reduction of the material hardness, which is much lower than expected. The present work provides a careful analysis of the range of the possible stable configurations for heavy transition metal carbides. Furthermore, this study may inspire further experiments on this promising class of materials at ambient conditions.

2 Computational methods

The CALYPSO code has been employed to predict the structure of Ru_2C at ambient conditions, and the underlying *ab initio* structural relaxations were performed using density function theory (DFT) with the Perdew-Burke-Ernzerhof (PBE) exchange-correlation functional in the generalised gradient approximation (GGA) [23]. A projected-augmented wave (PAW) method [24] was used as implemented in the Vienna ab-initio Simulation Package (VASP) [25,26]. Within PAW, $4p$, $4d$, and $5s$ states were treated as valence states for Ru; $2s$ and

$2p$ for C. For the structure searching, an energy cutoff of 650 eV and a Brillouin zone sampling grid with the resolution of $2\pi \times 0.05$ Å^{-1} were used. The obtained structures were re-optimized more accurately with denser grids, whose resolution was achieved at $2\pi \times 0.003$ Å^{-1}. A convergence till 0.001 meV was considered for the electronic problem, while the forces were relaxed to a value below 1 meV/Å. The electronic structure was calculated by using the Monkhorst-Pack **k**-grids [27] of $17 \times 17 \times 3$ points for both structures. To test the dynamical stability of the system, PHONONPY [28] was employed within density functional perturbation theory (DFPT) implemented in VASP. In DFPT calculations, a $4 \times 4 \times 4$ super cell consisting of 192 atoms for the $R3m$ phase and a $3 \times 3 \times 3$ super cell consisting of 162 atoms for the $R\bar{3}m$ phase were constructed to calculate phonon dispersion relations. The mapped **k**-mesh consisted of $5\times5\times5$ points. To ensure a reasonable convergence, an energy cutoff of 700 eV with a precision of 1×10^{-8} eV was pursued. The hardness of structures was calculated using the model proposed by Šimůnek and Vackář [29]. Our theoretical X-ray diffraction patterns were obtained using POWDER CELL code [30] simulations with *ab initio*-derived structural data (atomic positions, lattice parameters) as an input. The simulations assumed Mo-K$_{\alpha1}$ radiation and Bragg-Brentano geometry, which remains the same parameters with the experimental data (direct measurements in Ref. 12).

3 Results and discussion

3.1 Predicted structures and their characteristics

To begin we present the predicted structures in the rhombohedral axes. For the $R3m$ structure, the lattice constant a is equal to 5.29 Å, and the angle between the axises is equal to 30.35°. The Ru atoms are located at two $1a$ positions of (0.1333, 0.1333, 0.1333) and (0.3166, 0.3166, 0.3166), with the position of C atom at (0.8935, 0.8935, 0.8935). For the $R\bar{3}m$ structure, the lattice constant a is equal to 10.62 Å, and the angle between the axes is equal to 14.93°. The Ru atoms are located at two $2c$ positions of (0.6328, 0.6328, 0.6328) and (0.7704, 0.7704, 0.7704), and C atoms reside at $2c$ position with (0.4777, 0.4777, 0.4777). In the following discussions, instead of the rhombohedral representation, the hexagonal unit cells are used. The hexagonal unit cell of the $R3m$ phase contains three formula units, as shown in Fig. 1a, with a=2.77Å, c=15.14Å having a c/a ratio of 5.46. This structure is a clearly-cut layered structure, and a monolayer of C sandwiched by two layers of Ru atoms forms the periodic element showing $P\bar{6}m2$ symmetry in the unit cell. Each layer is displaced (1/3, -1/3, 0) with respect to its neighbouring layers. The hexagonal unit cell with $R\bar{3}m$ symmetry, shown in Fig. 1b, contains six formula units and has a very large c/a ratio of

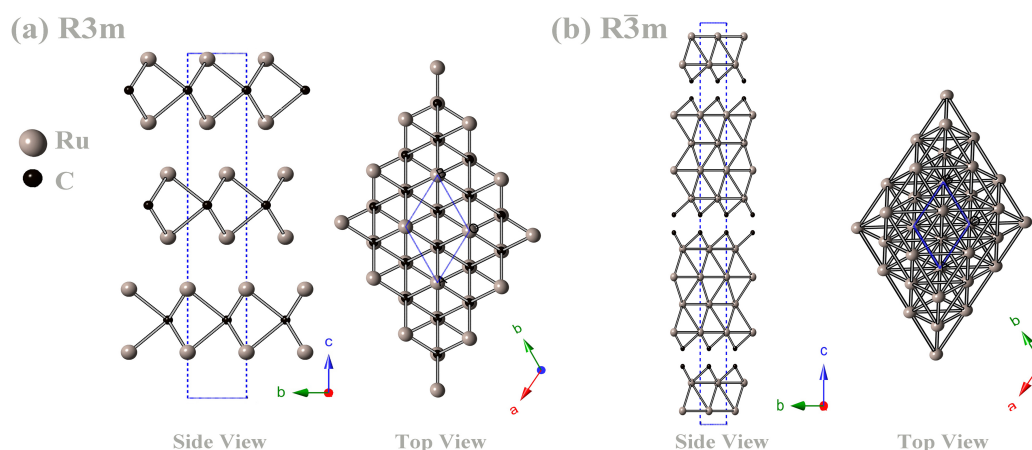**Fig. 1** The structure of the $R3m$ phase (a) and the $R\bar{3}m$ phase (b) in the hexagonal representations. For each of them, the side and top views are reported from left to right. The blue dashed lines denote the unit cell of Ru_2C. The Ru atoms are represented as big grey balls, while C atoms are represented as smaller black balls.

11.41. In the $R\bar{3}m$ structure, the lattice constant a is equal to 2.76 Å, and c reaches 31.50 Å. Overall, the structures of Ru_2C are constructed by stacking Ru or C layers along $\langle 001 \rangle$.
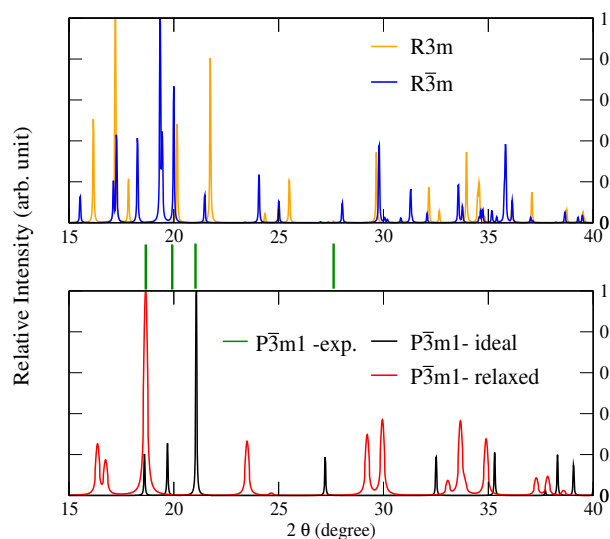

Fig. 2 Simulated XRD patterns of the predicted $R3m$ (blue line) and $R\bar{3}m$ (red line) structures, and the speculative $P\bar{3}m1$ structure (black line). The conditions are constrained at ambient temperature and pressure.

Let us first describe the two predicted rhombohedral structures. We emphasise that the $R\bar{3}m$ phase, as shown in Fig. 1b, is the structure with the lowest energy having the formation energy of 0.619 eV/f.u. We should note that instead of graphite, diamond structure is used here as the reference state for C to calculate the formation energy of Ru-C compounds.

This is because GGA cannot accurately reproduce the c-axis lattice constant and interlayer binding energy of graphite[31,32]. Given that the purpose of our work is to evaluate the formation energy of Ru_2C with respect to graphite as reference state of C, one can apply the energy shift from diamond to graphite obtained from more accurate exchange-correlation functionals, i.e. the dispersion corrected functionals[33–35]. Moreover, the graphite-diamond energy difference is rather small compared to the formation energy that we computed. Thus, it is emphasised that this will not change the conclusions but only change the absolute value of the formation energy. The $R\bar{3}m$ phase is the most energetically favoured structure. The $P\bar{3}m1$ structure assumed on the basis of the experimental data has a formation energy of 1.377 eV/f.u., while the $R3m$ phase has a formation energy of 0.921 eV/f.u. Thus all the three phases have positive formation energies with respect to hcp Ru metal and diamond. This is in full agreement with Ru-C phase diagram showing that a mixture of Ru metal and graphite is the equilibrium state of the system at ambient pressure and temperature[36,37]. From Fig. 1, it is also clear that Ru layers and C layers do not tend to mix evenly in the $R\bar{3}m$ structure, where the tetra-layers of Ru are separated by bilayers of C. In addition, the long-range order in the layered structure reminds us of the intercalation compounds, where the staging phenomenon is present by a periodic sequence of intercalated layers in the host matrix (metallic layers in general). It was reported that the atoms in intercalated layers may diffuse into the host matrix to form the disordered structure[38]. It is commonly recognised that a large amount of C vacancies exist in most of TMCs/TMNs, and this phenomenon is likely to occur in Ru_2C as well. Therefore, the study of the phase transition between the ordered and disordered structures is plausible in

the future and this work is rather beneficial for the study of phase diagram at various temperatures/pressures [39].

In the literature, no stable structures have been reported at ambient conditions for the late $4d$ or $5d$ TMCs/TMNs. Re_2C and Re_2N [11] are the high-temperature stable phases, and can provide some insight on the structures of the heavy TMCs/TMNs. The structure of $Re_2C(N)$ ($P6_3/mmc$) is composed of bilayers of Ru atoms and monolayers of C, while the Re_3C ($P\bar{6}m2$) structure is constructed of tri-layers of Ru and monolayers of C. It can be seen that the number of atoms corresponds to the number of layers for both Re-C and Ru-C systems. As a matter of fact, our predicted structure is analogous to this type of stacking. In the case of one formula unit, the structure of the $R3m$ phase shows the same type of stacking as Re_2C/Re_2N, i.e. bilayers of Ru and monolayers of C (2 Ru: 1 C). If we consider two formula units, instead, the $R\bar{3}m$ phase is constructed of tetra-layers of Ru atoms and bilayers of C atoms (4 Ru: 2 C). This one directional arrangement of TMs and C layers follows the rules of growth common for TMCs/TMNs. To shed some light into the formation mechanism of Ru_2C, let us compare the inter-layer distances in the predicted structures, and these values can be compared with hcp Ru metal and graphite. The inter-layer distance between Ru layers in the $R\bar{3}m$ phase is 2.16 Å, and the distance between C bilayers is 1.40 Å. The inter-layer distance of Ru layers in the $R3m$ phase is 2.27 Å. In the case of hcp Ru metal, the distance between Ru layers turns out to be 2.14 Å, which is rather close to the values in the predicted structures. Moreover, the inter-layer distance between Ru layers in $R\bar{3}m$ phase is almost the same. Inspection of the inter-layer distance within the C bilayers in the $R\bar{3}m$ phase shows that it can be approximately considered to be constructed of hcp Ru metal and graphite owing to the inter-layer distance of the C bilayers in graphite being of 1.40 Å (in-plane). It is known that the C-C bonds in graphite is sp^2 bonding, while the forming of bonds of C bilayers in $R\bar{3}m$ phase should differ from the C-C bonds in graphite owing to the participation of Ru layers. The distinctive distances of Ru and C layers in these two phases may alter the typical p-d hybridised covalent bond (see further discussion below).

The XRD patterns can be simulated from the relaxed structures and compared with the experimental data. In the lower panel of Fig. 2, the simulated pattern agrees with the four experimental peaks if the experimental data is assumed, where the ideal coordinates of Ru, C atoms are used. As the equilibrium volume at the ambient conditions in theory is greater than that of the ideal structure, the three peaks around 20° of the relaxed experimental structure show a clear shift towards lower angles. The XRD patterns of the $R3m$ and $R\bar{3}m$ structures are shown in the upper panel of Fig. 2. The peaks of the two structures show similar features and coincide at 17.2°, 20.1° and 29.8° with only a subtle shift of angles. More impor-
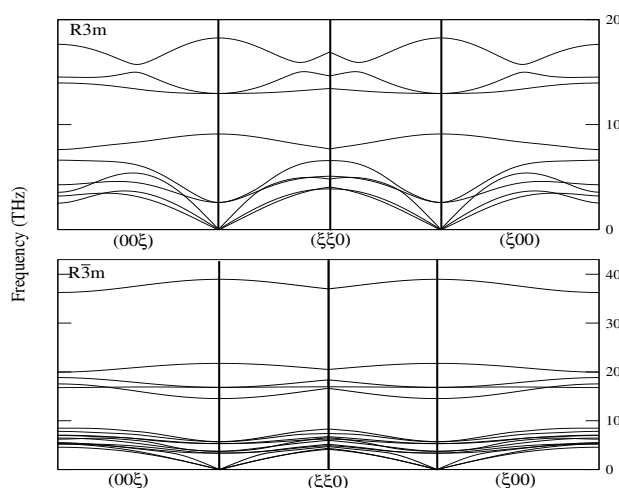

Fig. 3 The phonon dispersion curves (PDCs) of the $R3m$ and $R\bar{3}m$ phases of Ru_2C at ambient conditions. The phonon dispersion curves expand along the direction of (00ξ)-($\xi\xi$0)-(ξ00).

tantly, the diffraction pattern of $R\bar{3}m$ structure and the relaxed $P\bar{3}m1$ structure share certain similarities, and they can be even matched below 20° if a certain amount of shift is allowed. In reality, the shift of angles for the possibilities of matching in the diffraction patterns can be induced by the formation of defects or temperature/pressure effects. Lastly, the absence of experimental data above 30° made it impossible to extend our comparison. In brief, it is concluded that the computed diffraction patterns of the two structures can be used as a reference for future comparisons in both theory and experiments.

3.2 Dynamical stabilities and electronic structure

In addition to the structural properties, the dynamical stability is essential in order to judge whether the predicted structures are stable or not. In Fig. 3, the phonon dispersion curves (PDCs) of the $R3m$ and $R\bar{3}m$ structures at ambient pressure are reported. As we can see from the calculated frequencies, all the phonon modes are positive, indicating that the two structures are dynamically stable at ambient conditions. An interesting feature in Fig. 3 is that the $R\bar{3}m$ structure shows much more dispersive PDCs. The spectra contain states up to 40 THz, while only 20 THz are reached in the spectrum of the $R3m$ phase. The high frequency modes can be attributed to the strong covalent bonds between C bilayers in the $R\bar{3}m$ structure (see further discussion). Our results point to that the predicted two sandwich-like structures of Ru_2C are both dynamically stable.

The band structure and density of states (DOS) of Ru_2C are shown in Fig. 4. It should be noticed that values in DOS are reported in arbitrary units, i.e. they were rescaled to magnify the peaks. The curves reported in Fig. 4 show that our
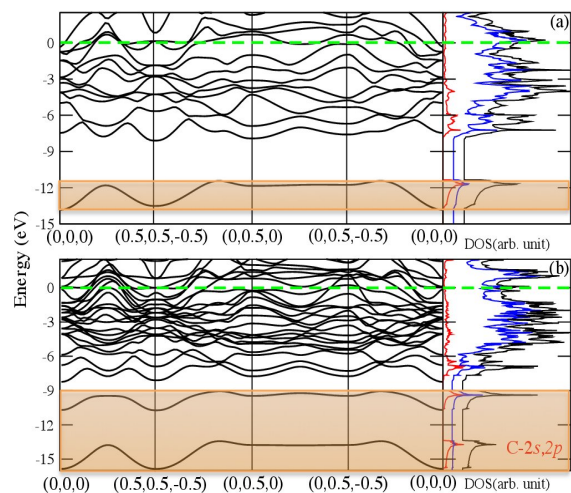
Fig. 4 Band structures and density of states (DOS) of the $R3m$ (a) and $R\bar{3}m$ (b) phases. The Fermi energy E_f is set to be 0 eV, and is indicated by the green dotted line. Inside the DOS plots, the red line refers to the contributions of the C-2p states, the blue line to the contributions of the Ru-4d states, and the black line to the total DOS per unit cell. The orange rectangles highlight the lower lying bands below -9 eV.

two phases of Ru_2C are metallic in nature, which is in agreement with the character of the $P\bar{3}m1$ phase[12,13]. The DOS around the Fermi energy E_f is mainly dominated by the 4d-states of Ru for both cases. The strong hybridised states are found around -4 eV in $R3m$ structure, and the broader peak can be identified around the same energy scale in the $R\bar{3}m$ structure. Another hybridised states can be found below -6 eV for both structures. In fact, the 4Ru-2C layered structure, namely $R\bar{3}m$ structure, weakens this hybridisation due to the less shared electron between Ru-C due to the strong C-C covalent bonds as well as the connection with the metallic Ru atoms. It is interesting to observe a gap between the upper valence band and the lower valence band marked in the orange rectangles. The band gap in $R3m$ structure is 3.22 eV, which is much larger than 0.76 eV in $R\bar{3}m$ structure. The C bilayer in $R\bar{3}m$ structure, i.e. the "mechanical joint" of Ru-C, can influence the lower lying energy level. It is emphasised that the splitting of the lower valence band with a gap of 2.56 eV is observed in $R\bar{3}m$ structure. Clearly, the lower valence band is mainly contributed by C-2s,2p states, and the band below the band gap in both cases are composed of Ru-C states (see further discussions). Briefly, it is clear that the band structures of the two phases are very similar. However, the primary difference lies in the position of the Fermi energy E_f, and that in the $R\bar{3}m$ phase several flat bands cross E_f and the the lower

valence band is split.

3.3 Chemical bondings and mechanical properties

Table 1 The charge imbalance per atom from Bader charge analysis. The positive (negative) sign denote the loss (gain) of electrons. There is no value for the charge of the type II Ru atom in the $R3m$ phase, due to that there is only one type of Ru atom there.

Strcuture	$Ru_I(e)$	$Ru_{II}(e)$	$C(e)$
$R3m$	+0.37		-0.74
$R\bar{3}m$	+0.42	-0.02	-0.40

Due to the differences in the electronic structure between the $R3m$ and $R\bar{3}m$ phases, one should investigate if these differences reflect into major changes in the nature of the chemical bonding. Therefore we analyse the Bader charges[40] and the electron localisation function (ELF)[41] in details, which are respectively reported in Table. 1 and Fig. 5. It can be seen that in the $R3m$ phase, each Ru atom loses 0.37 charge units and each C atom gains 0.74 charge units. In the $R\bar{3}m$ phase, one more type of Ru atoms (Ru_{II}) is found, which retains an almost unaltered charge during the formation process. The different types of Ru atoms can be better seen in Fig. 5, where the ELF is reported as well. In Fig. 5b, describing the $R\bar{3}m$ phase, the the Ru atoms at the boundary are of type I, while the inner bilayers of Ru atoms inside the quasi-rectangle are of type II. The small shift of charges observed in the Ru atoms of type II suggests that they are closer to the metallic nature. The larger loss of the charge of Ru_I in the $R\bar{3}m$ phase reveals that there is less covalency in comparison with the $R3m$ phase, and this phenomenon is in accordance with the DOS shown in Fig. 4. The amount of charge gained by the C atoms in the two structures is different as well. The carbon atoms in the $R3m$ phase obtain almost twice as much charge as in the the $R\bar{3}m$ phase due to the 'frozen' Ru_{II} atoms. As seen above, the connections between the Ru layers is built through the C monolayer for the $R3m$ phase and the C bilayer for the $R\bar{3}m$ phase.

Introducing extra atoms may lead to different chemical bondings. As shown in Fig.5a, the charges in the $R3m$ phase are very localised around the carbon atoms, while the clouds around Ru atoms are more spread leading to the formation of dumbbell shaped clouds, which indicates the covalent bonds. In contrast, a weak covalent bond forms between Ru-C in the case of the $R\bar{3}m$ phase (see Fig.5b), where the Ru-C-Ru is replaced by Ru-(C-C)-Ru. It is clear that a strong C-C bond in the $R\bar{3}m$ phase is formed and this can explain the split bands of C-2s. In the band structure plot (Fig.4b), the band at -9 eV is the anti-bonding states and the band at -13 eV is the bonding state. The low ELF regions between Ru_{II} atoms emphasise the delocalisation of charge in the $R\bar{3}m$ phase. Thus, the com-

bination of charge imbalance in Table 1 and ELF in Fig. 5, makes us conclude that the Ru_{II} atoms form metallic bonds. The metallic bonds for Ru atoms together with strong covalent bonds in C bilayers stabilise the $R\bar{3}m$ phase. Thus, the distinct number of Ru/C layers for the two phases accounts for the different nature of their chemical bondings.

So far, diamond or the most recent nano-twinned diamond[42], are the hardest known materials. This is attributed to the tetrahedrally bonded sp^3 hybridised carbon atoms that form a three-dimensional network with high symmetry. A three-dimensional network of short and strong bonds is essential for the hardness of a material. In its absence, the material would fail to resist the load in some specific direction, e.g. graphite, which can be cleaved even by stirring in water. In this context, it is clear why the light element systems that can form short covalent bonds like B, C or N, are the most studied systems[43]. Some TMCs/TMNs are also expected to be superhard, which is based on the principle that these materials can combine the high compression resistance of TMs and the covalent bonding arising from carbon. According to this principle, which was proposed by Kaner *et al.*[4], some superhard materials were successfully synthesised. The Ru_2C has a ratio of species Ru/C of two, and it is therefore inevitable that Ru-Ru bonds are of metallic nature form. These bonds offer poor resistance to either plastic or elastic shape deformations. The calculated hardness of the $R3m$ structure is 29.3 GPa, even though there are uniformly distributed Ru-C bonds (and with a large density). The hardness of the $R\bar{3}m$ structure is even less, since the strength of the covalent Ru-C bonds is remarkably reduced by the clustering of carbon atoms and the metallic Ru layers. As it is known that the TMCs/TMNs are highly resistant to compression, it is particularly interesting to consider the bulk modulus of these two phases. The calculated bulk moduli of the $R3m$ and the $R\bar{3}m$ phases are 312 GPa and 304 GPa, respectively. These values are both smaller than the bulk modulus of Ru metal (320 GPa), which is in accordance with the tendency reported for Os_xC_y compounds with various stochiometries[44,45].

4 Conclusion

We have performed extensive first principles structure search for the ground-state structure of Ru_2C at ambient conditions. The $R3m$ and $R\bar{3}m$ structures were found to be the most plausible structures of Ru_2C, and both these structures are dynamically stable at ambient conditions. The $R\bar{3}m$ structure is the most energetically stable with respect to the $R3m$ and the $P\bar{3}m1$ structure. The predicted two structures share great similarities with the structures of Re-C/N systems. The remarkable similarities with the structures of other late TMCs/TMNs give strong support to our predictions. In the $R\bar{3}m$ phase, we have observed the appearance of metallic bonds, which are glued
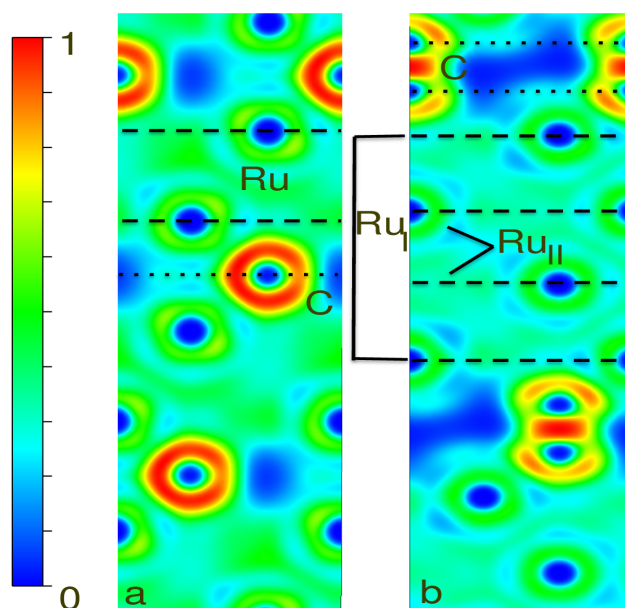

Fig. 5 The valence electron localization function (ELF) in the (110) plane of the $R3m$ structure (a) and $R\bar{3}m$ structure along the (110) plane, respectively. The dashed black lines represent the position of the Ru layers, while the dotted lines refers to C layers. In the case of the $R\bar{3}m$ phase, two different types of Ru atoms are labeled as Ru_I and Ru_{II}, which stand for type I and type II Ru atoms.

with the strong covalently bonded bilayer of C. The electronic structure reveals that Ru_2C at ambient pressure is stable in the metallic regime. In the $R3m$ structure, a much stronger $4d$-$2p$ hybridisation has been identified, and consequently the hardness is much higher than what is found in the $R\bar{3}m$ phase. In the $R\bar{3}m$ structure, the uneven distribution of Ru and C layers leads to a high concentration of Ru-Ru metallic bonds and weakens the Ru-C covalency.

5 Acknowledgments

References

1 H. Herchen and M. A. Cappelli, *Phys. Rev. B*, 1993, **47**,14193.

2   E. Knittle, R. M. Wentzcovitch, R. Jeanloz and M. L. Cohen, *Nature*, 1989, **337**, 349.

3   V. V. Brazhkin, A. G. Lyapin and R. J. Hemley, *Phil. Mag. A*, 2002, **82**, 231-253.

4   R. B. Kaner, J. J. Gilman and S. H. Tolbert, *Science*, 2005, **308**, 1268.

5   H. Y. Chung *et al.*, *Science*, 2007, **316**, 436.

6   L. E. Toth, *Transition Metal Carbides and Nitrides*, Academic Press, New York and London, 1971.

7   H. O. Pierson, *Handbook of Refractory Carbides and Nitrides: Properties, Characteristics and Applications*, Noyes, Westwood, 1996.

8   S. T. Oyama, *The Chemistry of Transition Metal Carbides and Nitrides*, Blackie Academic and Professional, Glasgow, 1996.

9   E. A. Juarez-Arellano *et al.*, *J. Alloys and Compds.*, 2009, **481**, 577.

10 A. F. Young *et al.*, *Phys. Rev. Lett.*, 2006, **96**, 155501.

11 A. Friedrich *et al.*, *Phys. Rev. Lett.*, 2010, **105**, 085504.

12 N. R. Sanjay Kumar, N. V. Chandra Shekar, S. Chandra, J. Basu, R. Divakar and P. Ch Sahu, *J. Phys.: Condens. Matter.*, 2012, **24**, 362202.

13 W. Sun, S. Chakraborty and R. Ahuja, *Appl. Phys. Lett.*, 2013, **103**, 251901.

14 D. M. Deaven and K. M. Ho, *Phys. Rev. Lett.*, 1995, **75**, 288.

15 C. W. Glass, A. R. Oganov and N. Hansen, *Comput. Phys. Commun.*, 2006, **175**, 713-720.

16 N. L. Abraham and M. I. J. Probert, *Phys. Rev. B*, 2006, **73**, 224104.

17 Y. Wang, J. Lv, L. Zhu and Y. Ma, *Phys. Rev. B*, 2010, **82**, 094116.

18 Y. Wang, J. Lv, L. Zhu and Y. Ma, *Comput. Phys. Commun.*, 2012, **183**, 2063.

19 H. Liu and Y. Ma, *Phys. Rev. Lett.*, 2013, **110**, 025903.

20 L. Zhu, H. Liu, C. J. Pickard, G. Zou and Y. Ma, *Nature Chem.*, 2014, **6**, 644.

21 E. Zhao, J. Meng, Y. Ma and Z. Wu, *Phys. Chem. Chem. Phys.*, 2010, **12**, 13158-13165.

22 Q. Li *et al.*, *Phys. Chem. Chem. Phys.*, 2012, **14**, 13081-13087.

23 J. P. Perdew, K. Burke and M. Ernzerhof, *Phys. Rev. Lett.*, 1996, **77**, 3865.

24 J. P. Perdew and Y. Wang, *Phys. Rev. B*, 1992, **45**, 13244.

25 G. Kresse and J. Hafner, *Phys. Rev. B*, 1993, **48**, 13115.

26 G. Kresse and J. Hafner, *Phys. Rev. B*,1994, **49**, 14251.

27 H. J. Monkhorst and J. D. Pack, *Phys. Rev. B*, 1976, **13**, 5188.

28 A. Togo, F. Oba and I. Tanaka, *Phys. Rev. B*, 2008, **78**, 134106.

29 A. Šimůnek and J. Vackář, *Phys. Rev. Lett.*, 2006, **96**, 085501.

30 W. Krauss and G. Nolze, *J. Appl. Cryst.*, 1996, **29**, 301-303.

31 H. Rydberg *et al.*, *Phys. Rev. Lett.*, 2003, **91**, 126402.

32 H. Rydberg *et al.*, *Surf. Sci.*, 2003, **532-535**, 606.

33 S. Grimme, *J. Comp. Chem.*, 2006, **27**, 1787.

34 S. Grimme, J. Antony, S. Ehrlich, and S. Krieg, *J. Chem. Phys.*, 2010, **132**, 154104.

35 A. Tkatchenko and M. Scheffler, *Phys. Rev. Lett.*, 2009, **102**, 073005.

36 H. Okamoto, *Desk Handbook: Phase Diagrams for Binary Alloys*, ASM Int., Materials Park, 2010.

37 E. Fromm and T. E. Gebhardt, *Gasses and Carbon in Metals*, Metallurgiya, Moscow, 1978.

38 N. Daumas and A. Herold, *Seances Acad. Sci., Ser. C.*, 1969, **268**, 373.

39 D. P. DiVincenzo, C. D. Fuerst and J. E. Fischer, *Phys. Rev. B*, 1984, **29**, 1115(R).

40 RFW. Bader and CF. Matta, *J. Phys. Chem. A*, 2004, **108 (40)**, 8385-8394.

41 A. D. Becke and K. E. Edgecombe, *J. Chem. Phys.*, 1990, **92**, 5397.

42 Q. Huang *et al.*, *Nature*, 2014, **510**, 250-253.

43 O. Knotek, R. Breidenbach, F. Jungblut and F. Löffler, *Surf. Coat. Tech.*, 1990, **43-44**, 107-115.

44 Y. Wang, M. Arai and T. Sasaki, *Appl. Phys. Lett.*, 2007, **90**, 061922.

45 C. Pantea *et al.*, *Acta mater.*, 2009, **57**, 544.